ENSO, CLIMATE VARIABILITY, AND THE RAPANUI, PART II. OCEANOGRAPHY AND RAPA NUI

Ferren MacIntyre
Oceanography
National University of Galway, Ireland

REVIEW OF PART I, THE BASICS

In Part I (MacIntyre 2001) we covered, or should have covered, the following points:

- The El Niño/Southern Oscillation phenomenon appears to have been a part of the coupled ocean-atmosphere circulation as long as there has been a Pacific Ocean.
- It is a consequence of planetary rotation and equatorial dynamics.
- Equilibrium oceanic motions tend to be circular (except at the equator), and persist because the ocean is essentially frictionless.
- ENSO is influenced by the Madden-Julian Oscillation (MJO), which is caused by the migration of the Indian Ocean's atmospheric convection center (Madden and Julian 1971, 1972).
- ENSO is affected by the Indonesian Throughput (highly variable surface flow between the Indian and Pacific Oceans), and to a lesser extent, by events in the Southern Pacific Ocean because of the annual northward displacement of the atmospheric equator to the InterTropical Convergence Zone (ITCZ).
- Conditions in the central gyres affect ENSO in later years because water downwelled by the curl of the wind stress moves toward the equator.
- ENSO has a direct influence on interdecadal climatology and the Earth's heat balance through changes in the Eastern Pacific Cold Tongue – which is the dominant site of heat uptake by the ocean.
- ENSO is closely coupled to the migration of the eastern front of the West Pacific Warm Pool,
- And to the accompanying movement of the Walker Convection Center, which is the principal route of water vapor into the stratosphere and the locus of rainfall sufficient to reduce surface salinity significantly.
- In its normal (non-ENSO) western position, the cumulonimbus of the Walker Convection Center make Singapore the city most frequently struck by lightning.
- Equatorial dynamics can often be reduced to long-wavelength wind-induced waves, invisible to the bystander, in which the water above the thermocline moves coherently. Kelvin waves move eastward at the equator at 2 m/s, crossing the Pacific in a couple of months. At the eastern boundary, they generate a pair of coast-hugging, poleward, warm-water waves which affect the entire western seaboard of the Americas. They can be reflected westward as off-equator Rossby waves moving at 0.9 m/s. In rectangular equatorial models, Rossby waves convert to equatorward coastal waves at the western boundary, recombining at the equator to become another Kelvin wave. In the real world, this boundary is angled, irregular, and partly open, reducing reflection to possibly insignificant levels.
- Coriolis force makes Kelvin waves converge at the leading edge, deepening the thermocline by downwelling.
- ENSO affects distant areas largely by displacing the high-altitude jet streams.

The water waves we are most familiar with are phase waves: the shape of the surface moves as water particles trace out circular orbits whose radius decreases exponentially with depth. Ideally, there is no net water movement. A duck sitting on the surface traces out a vertical circle as the wave goes by, but is not carried along by the wave. Only energy propagates. (Breaking waves are special cases in extremely shallow water where the rules change). Surfers can move with a non-breaking wave, but they do so by sliding down its forward slope (extracting energy from the wave as it continually lifts them). A surfer could glide right by a sitting duck.

The homely analog of Kelvin and Rossby waves is water sloshing back and forth in a bathtub. Water itself moves from one end of the tub to the other. 'Seiches' in lakes occur when the wind pushes water to one end and then stops: the water sloshes back and forth a few times. In ENSO, the eastward slosh is along the equator (a fast Kelvin wave); the westward return is a pair of slower off-equator Rossby waves. (The detailed flow patterns differ because all the water in a bathtub moves along more or less semicircular paths. In the Pacific, a thin layer slides above the thermocline).

CONVECTION CENTERS, AND TELECONNECTIONS

The metronome of ENSO is the steady eastward drift of equatorial atmospheric convection centers. The natural position of a convection center is over the warmest water; drift displaces it (and the warmest water) in a quasi-regular manner. When it is far enough downstream, a new center regenerates in its home position, beginning the cycle again.

A familiar analog of this drift is the manner in which smoke from a bonfire follows a solitary bystander in the absence of a prevailing breeze. As in a convection center, ground-level air moves inward toward the bonfire from all directions. The bystander impedes flow from one direction; the net pressure is thus directed toward him – and so is the smoke. The similar pressure reduction at an equatorial convection site is caused by Coriolis force deflecting incoming winds, which are divergent from the east and convergent from the west, resulting in a net pressure eastward. Unlike the bonfire, the convection center itself is free to move, and does.

The boundary layer of the atmosphere (the lowest kilometer that is directly influenced by interaction with the Earth's surface) is full of cumulus clouds and thermals, which move heat from the surface to the atmosphere. Thermals, created by rising air too dry to produce a cumulus cloud (but beloved of soaring birds and glider pilots) carry only sensible heat. Moister rising air produces cumulus, and delivers the much larger latent heat from the condensation of water vapor.

Deep convection, provided by cumulonimbus which penetrate the boundary layer, is the principal mechanism by which the earth's surface temperature is communicated to the free atmosphere. Temperate-zone thunderstorms (associated with cumulonimbus) are frequent, but lack a permanent energy source at the surface and move with local weather systems. Deep atmospheric convection requires continuous energy input from a water surface with temperature above 28°C.

It appears that the matching but offset contours of Africa and South America so skew the equatorial Atlantic that its current system does not favor the development of an equatorial convection center. This same geographical skew delivers Atlantic equatorial heat energy into the North Atlantic, providing a hemispheric asymmetry to Atlantic hurricane generation.

Between the north-south asymmetry of the Indian Ocean and the resulting monsoon, its convection center never develops to the extent of the Pacific center.

All of this means that the Pacific's Walker Center is the single most important route by which solar heat input reaches the free atmosphere. Since the motion of the Walker Center is intimately connected with ENSO, it is not surprising that distant weather patterns (teleconnections) are also associated with ENSO. Only the seasonal cycle and the monsoon contribute more to weather variability than ENSO (Allan 2000).

Most known teleconnections are in the northern hemisphere. This is an artifact of land distribution: there are many more people living in the northern temperate zone than in the southern. Major changes in precipitation and wind patterns over the open ocean go largely unnoticed.

Having said all of the above, the mechanisms of weather variability remain mysterious. A recent book on the global effects of ENSO contains the wonderful sentence, 'El Niño and La Niña episodes of the ENSO phenomenon can be both synchronous and asynchronous with El-Niño-like and La Niña-like signals on various decadal to multidecadal timescales, resulting in permutations that lead to either enhanced or suppressed regional rainfall regimes'. Translation: 'We haven't a clue.'

The classical work on continental consequences of ENSO was the collation of historical (and largely anecdotal) data from South America by Quinn and Neal (1983a, 1983b). This work, and its reconsideration by Ortlieb (2000) provide the foundation for reconstruction of the past history of ENSO. This region lies so close to the equatorial Pacific that it hardly counts as a teleconnection, yet it provides a good temporal record of previous ENSOs. Someone familiar with 16th-19th century Rapa Nui history might find it interesting to compare notes with us.

THE OCEANOGRAPHIC SETTING

Temperature Sections

Figure 1 shows a late stage of the TOGA/TRITON moored-buoy array which has provided most of what we know about the conditions behind ENSO. The circles mark moored buoys with anemometry and thermistor chains (Hayes et al. 1983) and squares moored buoys with Acoustical Doppler Current Profilers or ADCPs. There were also drifting buoys (Niiler et al. 1995), tide gauges on many islands and shore stations, and expendable bathythermographs from ships of opportunity, supplemented by satellite imagery and sea-surface temperature (SST) estimates. The system developed slowly, so that early data (1985) is available only from a single line of buoys. Salinity, rainfall, and solar radiation sensors were later added to several TAO moorings in the west (Cronin and McPhaden 1998).

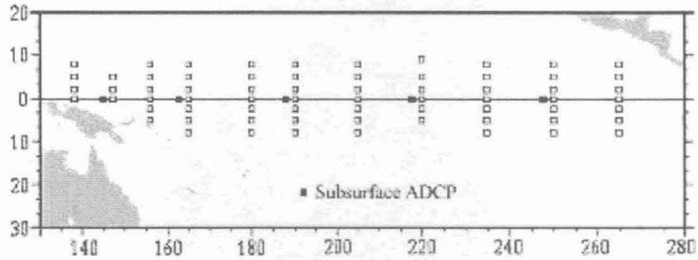

Figure 1. Deployment of remote-sensing buoys of TOGA at the end of the experiment in degrees of latitude and longitude. The hardware remains in place as the ENSO Observation System (after Kessler et a1. 1995).

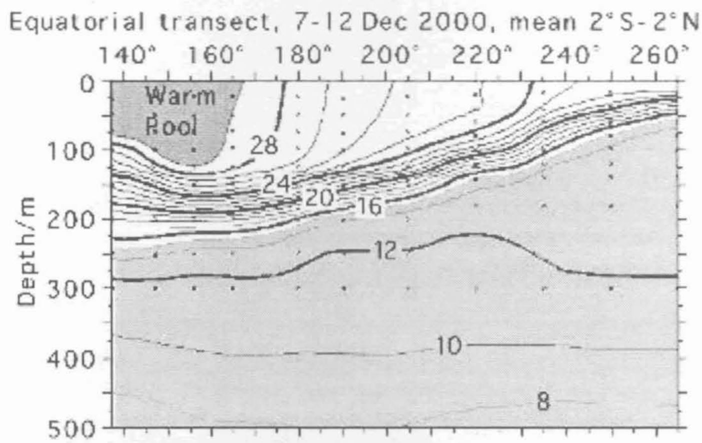

Figure 2. Temperature vs depth along the equator in a non-El Niño year. The tradewind-driven surface ultimately feeds into the Warm Pool in the west.

Figure 2 is a temperature transect of the equatorial Pacific in a neutral year, obtained from the TOGA moored-buoy array shown in Figure 1. The dark gray area at the western surface is the Western Pacific Warm Pool; which accumulates the water that will become an El Niño. The thermocline is the sloping band between 16° and 24° where the temperature changes most rapidly with depth. The thermocline rises from 200 m in the west to 50 m in the east, and this incline is reflected in a smaller reversed slope of the sea surface, which is often 40 cm higher in the west, as shown in Figure 2. The mean slope of the thermocline is on the order of 10-5, or 1 mm per football field. The gravitational force tending to flatten the thermocline is ultimately balanced by the wind stress at the surface, but not in any easily explicable manner: the equatorial current system is far from simple even in the absence of periodic ENSOs.

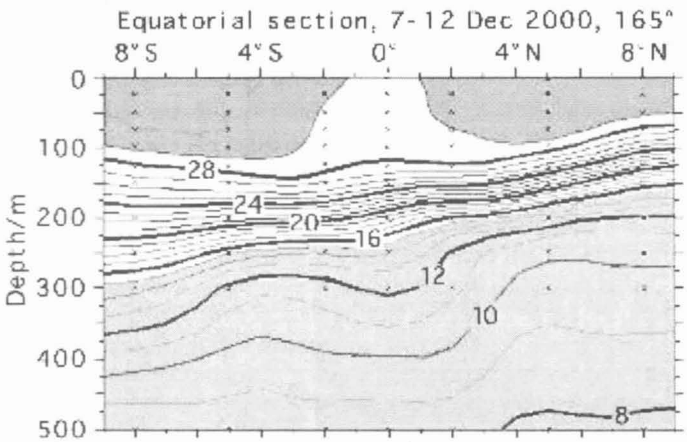

Figure 3. Temperature vs. depth across the equator at 165°E, synoptic with (observed at the same time as) Figure 2. The ideal ocean is symmetrical around the equator; the observed asymmetries are forced by the northern location of the ITCZ. (Graphs drawn by http://ingrid.ldgo.columbia.edu/.) The frictionless nature of the ocean means that the principal dynamical effect of the thermocline is to uncouple motions across it, allowing the warm water to move independently of the deep water.

Figure 3 is the transverse companion of Figure 2, showing the temperature structure near the western edge of the Warm Pool. Note three features: the N-S asymmetry caused by the northward displacement of the atmospheric equator, the slightly cooler water at the equator itself, which is a consequence of wind-driven upwelling, and the downward bulge of the 10° and 12° isotherms at the equator itself, which is a manifestation of the Equatorial undercurrent (EUC) – itself the first-order eastward return of water driven west by convergent trade winds.

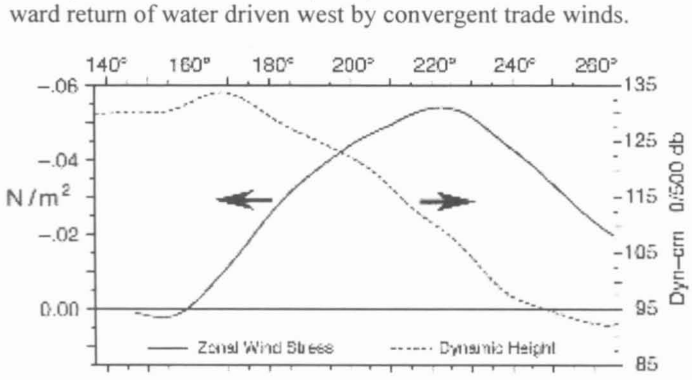

Figure 4. Mean zonal section (1988–1996; 2°N–2°S) of wind stress and dynamic height. Think of the right-hand scale as centimeters of sea-surface elevation. (After McPhaden et al. 1998.)

Figure 4 shows the remarkable ocean-wide average match between force (wind stress) and response (piling up of water in the west), but the local steepness of the topography at the edge of the Warm Pool is much larger than appears in Figure 4, which is reduced by averaging as the edge of the Warm Pool migrates as shown in Fig. 5. Most of the change in height occurs over a few hundred kilometers at the edge of the Warm Pool, which would be a step change on the scale of the figure.

Figure 5. Longitude-time distribution of isotherms between 4° N-4°S. The upper axis and the white line are the Southern Oscillation Index with a 6-month smoothing filter. El Niño events are the dark tails extending to the east. Black areas are >29°C, medium grey >28°, and light grey >26°. (After Picaut et al. 1996.)

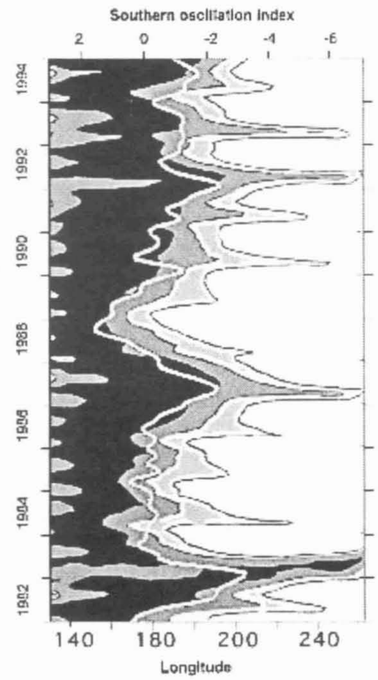

Figure 5 is a record of 13 years of TOGA data. Although the Southern Oscillation Index (SOI) is defined by a trans Pacific atmospheric pressure difference, its simplest oceanic descriptor is the latitude of the 28.5° isotherm of Figure 5, showing the close coupling in this two-fluid system. The black tongues leave a strong impression that El Niños occur by water spilling eastward from the Warm Pool, but complexities await.

As noted earlier, and as is obvious here, the period of the SOI is highly variable, with a broad peak in the power spectrum between three and seven years.

Velocities

Figure 6 offers an example of TOGA data near the edge of the Warm Pool at 165°E. The lines of constant salinity reflect the asymmetry of the equatorial system. If temperature and salinity were combined to show density, isopycnals (lines of equal density) would be far more symmetrical than the contours here, and would lie almost flat. The data are averaged over 917 profiles collected on 64 cruises over a 14-year period. The instantaneous flow pattern is so much at the mercy of variable driving forces that the real system never looks like the flows generated by computer models, and the net flow varies between ±50 Sv (Sv = sverdrup, or 106 m^3/s) (Johnson et al. 2000). (For comparison, the Gulf Stream in its early stages as the Florida Current runs at 30 Sv.)

The negative (westward) velocity at the equator is the wind-driven surface current; the central light area of high eastward velocity at 200 m is the Equatorial Undercurrent. Note the

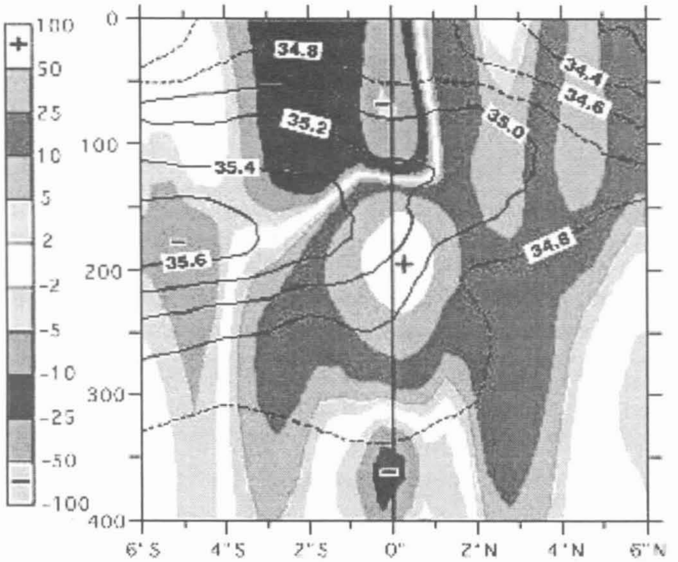

Figure 6. Salinity and zonal velocity (positive eastward, out of plane of paper) at 165°E, near the edge of the Warm Pool. The zonal velocities are relative to water at 700 m, assumed motionless for the sake of calculation. (After http://www.pmel.noaa.gov/ ~kessler/salinity/.)

complex subsurface velocity structure near the equator, and the asymmetry of the isohaline contours – both of which remain unexplained by theory, although ad hoc explanations can always be conjectured.

Figure 7 shows a time sequence of subsurface temperature anomaly during the 1997 El Niño. This gives the appearance of warm water being transported by the Equatorial Undercurrent (which lies in the thermocline). Yet I have discussed this with a number of people who have collected similar data, and one and all they talk in terms of Kelvin waves deepening the eastern thermocline, a process which warms the surface by depressing cool water below the reach of upwelling. Things are not as straightforward as they might seem.

The Warm (Fresh) Pool

The well mixed Western Pacific equatorial Warm Pool is fundamental to ENSO. For many purposes, the Warm Pool is best defined by its sea-surface temperature (SST) signature, as shown in Figure 2.

With little seasonal variation, most of its interannual variability is spatial and related to ENSO. Its eastern edge is a sharp salinity, temperature, and density front some 60-80 m deep, which oscillates 1500 km in either direction around its mean position at 170°E. During an El Niño it may extend eastward another 8000 km.

The heat balance in the Warm Pool is known only roughly from one 3-month sampling (Cronin and McPhaden 1998). Of the incoming 1350 watts/m^2 at the top of the atmosphere, only 150–200 make it to the ocean surface as incoming short-wave radiation, after averaging over day and night, reflection from clouds, and absorption in the atmosphere. 50 watts/m^2 leave as outgoing long-wave radiation. Heat storage may range between ±100 watts/m^2, going low during month-long westerly wind bursts when the sky is cloudy and hot water is leaving. Heat advected by surface currents changes from 75 to -25 watts/m^2 (output during westerlies). Minor amounts are lost to the thermocline, and as sensible heat to the atmosphere. Instead of a neat thermodynamic analysis of inputs and outputs, the net result of this study – as for so many studies of ENSO – was an appreciation of 'the complexities of [the] processes involved'.

A story known to all oceanographers is the mapping of the thermohaline (deep) circulation of the ocean by the Meteor expedition. The currents are too small to measure directly, and were deduced from measurements of pressure, temperature, and salinity, using one of the most elegant scientific tools ever invented: clever, precise, accurate, rugged, and inexpensive. This was a string of Nansen bottles (to capture water for salinity measurements), each carrying a pair of reversing thermometers. One is protected from ambient pressure and measures temperature, the other's mercury bulb is squeezed by water pressure and it measures a composite of temperature and pressure. When the string is lowered to depth, a weight is dropped. When it hits the top Nansen bottle, it releases a catch, allows the bottle to invert,

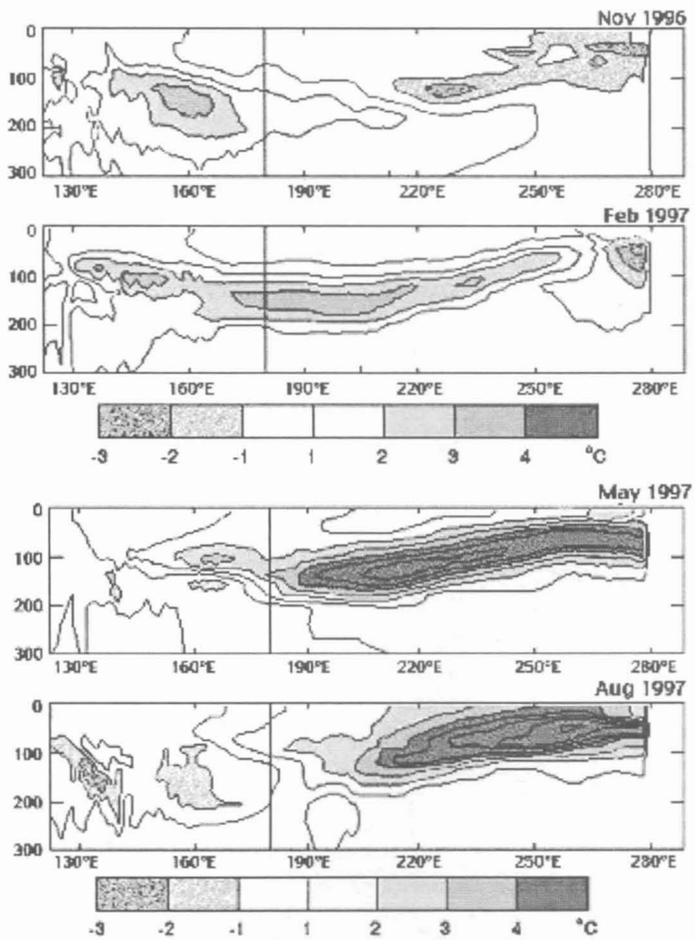

Figure 7. The time sequence of temperature anomaly during the 1997 El Niño. In August of 1997 the subsurface temperature anomaly reached 9° C. After Webster and Palmer (1997) from data provided by A. Leetmaa and M. Ji (National Center for Environmental Prediction. See also http://monsoon.colorado.edu/faculty/fig3full.gif.)

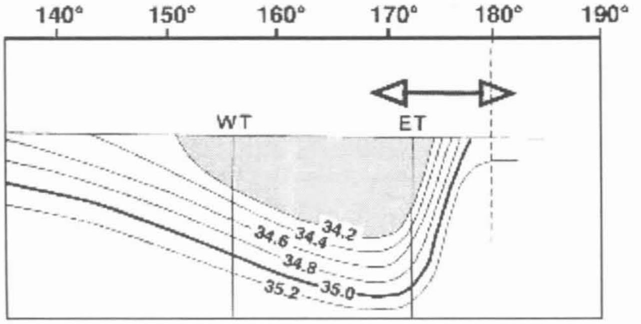

Figure 8. Idealized salinity structure of the Warm Pool, showing why this part of it is also called the 'fresh pool'. The double-headed arrow represents the normal (non El Niño) motion of the salinity front. (After Hénin et al. 1998.)

closing valves at top and bottom, precisely breaking the mercury thread in the thermometers, which thereupon store ambient data, and releasing another weight to trigger the next bottle deeper. The data allow the density field of the ocean to be mapped, and thence the pressure field, and thence the flow patterns. This works for the deep waters because conditions there change on a time scale of decades to millennia. The method is not well adapted to the erratic currents of the equatorial surface.

Nor is it possible to measure salinity accurately from the TOGA buoys: the sensor biofouls as organisms settle on surfaces, and its accuracy (which needs to be 1 part in 100,000) degrades in a matter of days if one can't clean and calibrate his instruments.

Abandoning hopes of applying classical T-S methods, there is still a bit that can be usefully said about salinity. The best picture we have of the salinity structure at the edge of the Warm Pool is that of Hénin et al. (1998), shown in Figure 8, which is reconstructed from data collected by ships of opportunity along the tracks WT and ET. The structure of Figure 8 is a quasi-steady-state system maintained by precipitation and currents. Rain continually recreates the 'fresh pool'; waves and turbulence continually blur its boundaries; currents continually compress and confine it. The currents that move the salinity front are driven by the zonal wind.

According to Cronin and McPhaden (1998), on the equator at 156° (not always under the convection center and heaviest rainfall), precipitation (4.5 m/yr) exceeded evaporation (1.4 m/yr) by 3.1 m/yr. The rainfall creates shallow short-lived puddles of fresh water which rapidly mix into surface water. The mean halocline is one unit of salinity over a depth of 100 m, a gradient exceeded only in estuaries. The atmospheric convection center both creates, and follows, the precipitation maximum (salinity minimum) in the Warm Pool, and thus lies about 5° west of (behind) the salinity front.

Table 1. Phases of the canonical El Niño. (-1) means the year before the fully developed El Niño. (After Harrison and Larkin 1998.)

Phase	Start	Through	Eastern Equatorial SST anomaly
Pre	May(-1)	Nov(-1)	Anomaly below significance
Ante	Dec(-1)	Feb(0)	Warming, but not significant
Onset	Mar(0)	Jun(0)	Significant anomaly; rapid increase
Peak	Jul(0)	Dec(0)	Maximum amplitude, little spatial evolution
Decay	Jan(+1)	Apr(+1)	Decreasing amplitude
Post	May(+1)	Aug(+1)	Anomaly below significance

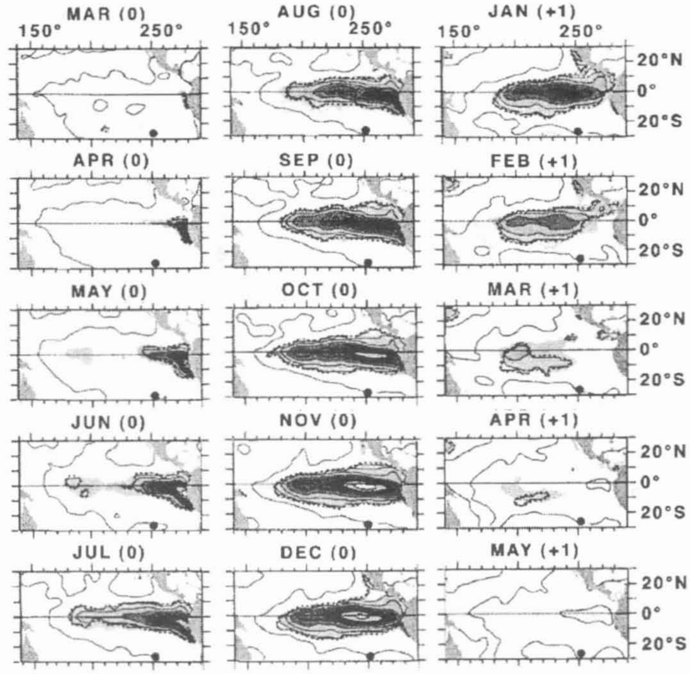

Figure 9. A simplified version of the evolution of the canonical SST anomaly. Rapa Nui is marked by a black dot: the line of zero effect passes through, or near, Rapa Nui in all months. Note the westward propagation of surface warming. (After Harrison and Larkin 1998.)

The Canonical El Niño

Creating the Composite

Harrison and Larkin (1998) create a composite El Niño by abstracting 36 elements of the 10 ENSO events since World War II (1946-1993). Of the 36, 24 are 'robust' (present in more than 5 events, absent in no more than 1) and five are 'not robust' (absent in more than one event). Four of the 'not robust' events are extra-Pacific and of no interest to us; the other will be discussed below.

They divide an ENSO event into the 6 phases of Table 1, distinguished by the statistical significance of the composite mean eastern equatorial SST anomaly averaged over 4°N–4°S, 252°–262°E, with 'significance' designated as ±0.62 standard deviations.

Recall that in Part 1 an 'ENSO year' started in October, which here is the center of the anomaly peak. This uncertainty over the best descriptors arises from real variability, the paucity of consistent climatological data, the lack of solid theory, difficulties of interpretation and differences in emphasis.

A common but not robust feature is that warm water first appears at the Peruvian coast in Nov(0) as in Figure 9, and spreads west, finally disappearing in the Central Pacific at Apr (+1). The direction of surface warming has little to do with the motion of warm water (which is always eastward), and everything to do with the depth of the thermocline, surface wind stress, upwelling, and local heating and cloud cover.

Harrison and Larkin also map monthly wind anomalies. During Pre there are westerly anomalies in the Indian Ocean whose center moves east from Sep(-1) through Nov(-1). Unfortunately, the authors mention neither MJO nor Walker events, but this eastward motion looks to me like migration of the MJO center. There are no wind anomalies during Ante. Weak westerlies show up at the end of Onset between 150° and 200°, and intensify throughout Peak. By the end of Decay they are gone. This looks like eastward migration of the Walker Center. Anomalies in meridional wind appear at 5°N in the east Pacific, suggesting that the ITCZ has moved toward the equator.

History of ENSO Hypotheses

Bjerknes (1966, 1969) – helped by video images from satellites – was the first to see that ENSO was a self-sustained coupling of two oscillating systems in which SST variations in the ocean produced wind changes in the atmosphere which in turn lead to the SST variations. As Bjerknes clearly recognized, coupled oscillators with different natural frequencies normally show complex patterns involving sum and difference frequencies, so one might expect irregular behavior from ENSO. Nevertheless, the then limited understanding of equatorial dynamics, and the absence of coupled models, gave rise to the mistaken idea that Bjerknes's approach should lead to permanent El Niño or La Niña conditions.

The Recharge Hypothesis

Wyrtki (1975) gave the first accurate description of the coupled changes in sea level, thermocline depth, and wind stress which are the preconditions of an El Niño. A fundamental feature was that the Warm Pool emptied to produce an El Niño and then had to be recharged.

Rasmussen and Carpenter (1982) added seasonal forcing to Wyrtki's hypothesis. Warm water appeared first at the coast and expanded westward. Barnett's (1983) empirical-orthogonal-function analysis of observations confirmed this approach.

Just when everyone was happy with this 'canonical' evolutionary scenario (Wallace et al. 1998), the largest El Niño to date occurred in 1982 – and misbehaved. Warm water appeared eastward out of the Warm Pool along the surface. Perversely, recognition of this event was delayed because satellite data was confused by simultaneous dust from the eruption of El Chichón. Data analysts rejected the perplexing SST signals and replaced them with climatological means. In situ data were rejected in turn because they disagreed with the published satellite data (McPhaden et al. 1998). [There is a moral here: Publish anomalous data, mention your inability to explain it, but don't discard it!]

SSBH Delayed-Oscillator Hypothesis

The 1982 event spawned new ideas about ENSO. McCreary (1985) found a way to sustain oscillations. His proposed mechanism involved the reflection of 'subtropical oceanic upwelling Rossby waves' at the western boundary of the Pacific equatorial waveguide.

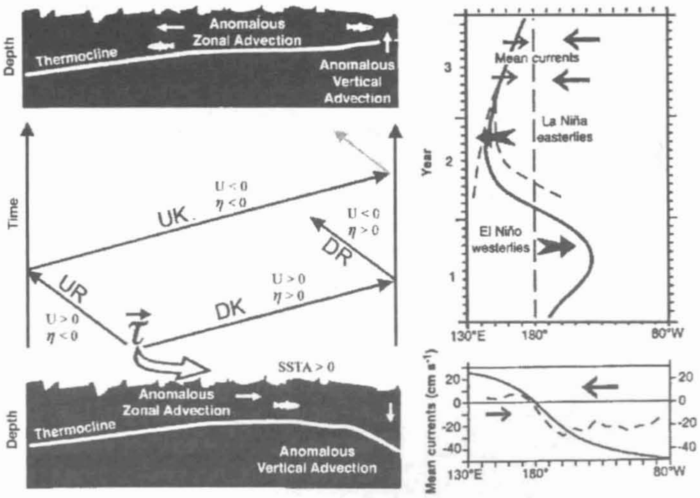

Figure 10. The coupled advective-reflective, or delayed-oscillator, theory of ENSO. A) t is the wind stress which drives the system. The heavy curve is the position of the convective center. UK and DK are the positive and negative Kelvin waves, UR and DR the Rossby waves. (After Picaut et al. 1997.) B) The dashed lines are the tracks of drifters moving toward the eastern edge of the Warm Pool. Eastward of the pool drifters move out of the equatorial trap, reaching poleward velocities of 5 cm/sec. (After Delcroix et al. 2000).

Battisti (1989), Schopf and Suarez (1988), and Battisti and Hurst (1989), refined McCreary's approach into the 'delayed-oscillator' theory of Figure 10. Recall (MacIntyre 2001:Figure 8) that as the easterly wind piled up westward-moving Rossby waves off equator, it also dug a hole on the eastward equator. Somewhat confusingly, this hole is known as a 'downwelling Kelvin wave' (DK in Figure 10), and it travels eastward while the 'upwelling Rossby wave' (UR in Figure 10) travels west. (We pointed out earlier that westerly winds moved the Warm Pool eastward, and because Coriolis force caused them to converge, they forced water downwards at the front of the Warm Pool. According to established usage, an Upwelling Kelvin wave, moving eastward, downwells water to deepen the thermocline. (My attempts to persuade equatorial oceanographers to adopt clearer usage – even when I offered them equally obscure neo-Greek adjectives to conceal their art from hoi polloi – were soundly rebuffed. They know what they mean!)

According to SSBH, an initial positive perturbation of the SST in the eastern equatorial Pacific generates a westerly wind in the western Pacific, which in turn increases the SST anomaly by deepening the thermocline, thus producing a full-fledged El Niño. Meanwhile, the system generates upwelling Rossby waves, which move westward (outside the equatorial waveguide) at -0.9 m/s. When these arrive at the western boundary, they reflect as Kelvin waves, The round trip takes about nine months. West winds amplify eastward-moving Kelvin waves, restoring any energy they may have lost in transit and reflection. When the Kelvin waves reach the eastern SST anomaly, they suppress it; after 2 or 3 cycles, El Niño subsides and normal conditions are restored in the east. In such models, removal of the western boundary suppresses El Niños entirely Kerr (1999).

This may have been the leading theory of ENSO for the next decade, but it has flaws (Picaut et al. 1997). It places the driving focus of ENSO in the eastern instead of the central Pacific (McPhaden and Picaut 1990), with the maximum wind-stress field 20° to 40° too far east (Mantua and Battisti 1995). As reflectors go, the western boundary of the Pacific – consisting of randomly placed islands with randomly oriented shorelines – looks more like the wall of an anechoic chamber, designed to absorb energy and break an arriving disturbance into multiple incoherent reflections (Verschell et al. 1995, Kessler and McPhaden 1995). In contrast, the eastern wall, oriented N-S, nearly smooth, and rising steeply from deep water, is not a bad reflector.

Kessler (1991) suggests that reflected Rossby waves cannot make a significant contribution to Kelvin waves in the real world. The reflected Rossby waves were apparently introduced only to account for the timing of El Niños, but there seem to be other ways to account for timing.

Penland and Magorian (1993) claim that linear advection of SST (by Pacific Kelvin and Rossby waves) is not sufficient to account for dynamic behavior during El Niño, leaving room for additional transport mechanisms. One such is that the strongest seasonal signal near the Walker Center is the Indian Ocean monsoon (essentially a large land/sea breeze oscillation as the Tibetan Plateau warms and cools). Superimposed on this is the shorter MJO cycle. The eastward drift of the Indian Ocean convection center may bring warm water out of the Indian Ocean through Australasia to join the Walker Center and urge it eastward also. The process repeats on a 30 to 90-day cycle, but it appears that passage through Indonesian waters is so variable that MJO's contribution to ENSO is nearly random.

Indonesia has only recently had professionally trained native oceanographers, and they are just beginning to study the complicated transport that comprises the Indonesian Throughput. Give them another decade, and we may understand ENSO a great deal better.

Triggering of El Niño

We have already dismissed the initial hypotheses of El Niño triggering. The westerly wind bursts are a common feature of the preliminaries (Luther et al. 1983), and the reflected Rossby waves probably don't reflect after all.

Delecluse et al. (1998) raise the interesting question of bidirectional teleconnections, asking whether these distant phenomena feed back into the ENSO cycle. If so, there are a number of possible remote triggers, but no mechanism has been proposed, let alone demonstrated.

My feeling is that Kelvin waves are quasi-periodically generated by the movement of convection centers – and that this is most of what is needed. The periods of the MJO and Walker cell are different, unrelated, and perhaps incommensurable.

However, the very name 'El Niño' indicates that there is some mode locking in the system; this occurs when the natural frequency of one system is a multiple of the other's frequency. A familiar example is walking with a small child, who must take two steps for the adult's one, thus mode locked at a frequency ratio of 1/2. Speed up a bit, and the child has to trot to keep up, no longer in step.

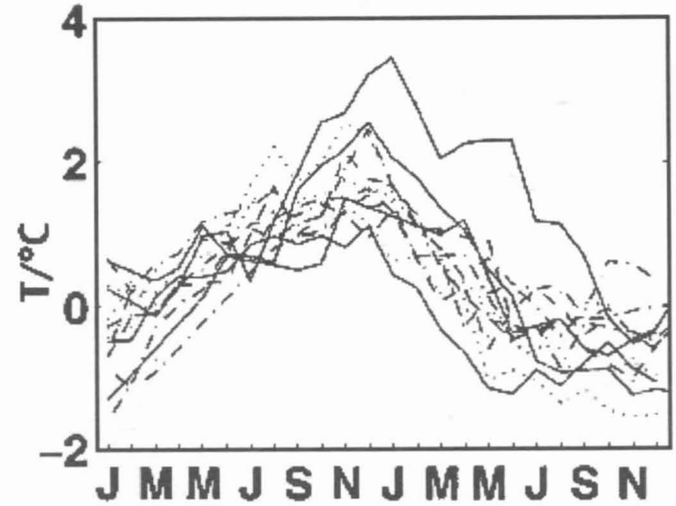

Figure 11. Mode locking of El Niños. In the years an El Niño occurs, it is most often seasonally mode locked. The 2 strongest seasonal signals associated with El Niños are the monsoon and the annual migration of the ITCZ, but their relation to triggering is only conjectural (after Tziperman et al. 1996).

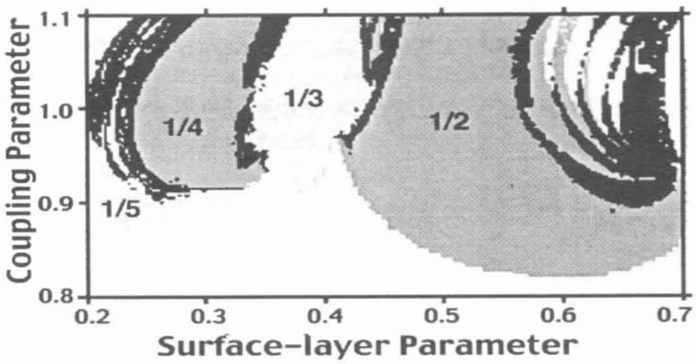

Figure 12. An example of chaos in ENSO, from model calculations. The gray regions indicate mode-locked behavior at the indicated frequency ratios. The black regions go chaotic. (after Jin et al. 1996.)

Figure 11 shows 13 episodes from 1888 to 1982 which peaked around Christmas (but not every Christmas), omitting non-Christmas events in 1957 and 1977, and the intense El Niños from the 1990s, whose timing may be affected by rising global temperature.

Mode locking indicates that there is a strong seasonal component to the trigger (Tziperman et al. 1997). Figure 11 suggests that triggering occurs a year before El Niño peaks, and also that once it begins, events of the next year are pre-ordained. Does the winter equatorward movement of the ITCZ – which brings symmetry to equatorial planetary wave – trigger the following winter's El Niño?

Chaos and Nonlinearities

The simplest hydraulic system which behaves a bit like

ENSO is a dripping faucet (Shaw 1984). For low leakage rates, the drip frequency is constant; increase the leakage, and the drip may become unpredictable (chaotic). Other important variables are the diameter and shape of the orifice, the size of the low-pressure reservoir downstream of the constriction, and even trace amounts of surface-active materials in the water. Because of non-linear feedbacks in the flow pattern, the system shows sharply limited predictability even if the starting conditions are known.

Mode locking occurs in the gray regions of Figure 12, which shows the behavior of a coupled air-sea model of intermediate complexity. The exact definitions of the axis parameters are model dependent: the important aspect is the black areas of chaotic behavior which separate the mode-locked regions. I suspect that if the two frequencies are themselves irregular, the chaotic domains of Figure 12 grow dramatically. The real system appears to live in one of these cracks, where seasonal forcing is not strong enough to keep Warm Pool formation and draining in step.

Non-linearity in the ENSO system arises inter alia from the vagaries of weather, where Lorenz (1963) first recognized that chaos was an inescapable part of the mathematics.

The ENSO Cycle

It is useful to have a working model of ENSO, even if it is not entirely correct. What follows may be a straw man, sturdy enough to stand up by himself, but easily pushed aside by better data or theories. One can at least base intelligent questions on it.

Filling the Warm Pool

The Indian and Pacific Oceans organize their atmospheric equatorial convection cells differently.

1) The trans-Pacific fetch of easterly trade winds drives warm water off the equator to become westward-moving Rossby waves, transporting heated water westward. The water absorbs solar heat as it travels.

2) The normal position of the Pacific equatorial atmospheric convection center (the Walker Center) is in the west, over the warmest water.

3) As water temperature rises above 28°C, the Warm Pool initiates the deep stratospheric convection which is the upward branch of the Walker cell. The surface winds drive the convection center eastward, extending the Warm Pool.

4) Convection over a warm pool is stable. Convection over a warm line is not. Cloud shadows matter. One expects some indecision about migration of the convection center as it moves eastward far enough to allow a 2nd cell to regenerate in the west.

5) If all goes well, the Walker cell and leading edge of the growing Warm Pool migrate together toward the Date Line.

6) The warm water behind eventually generates sufficient convection to interrupt westerly winds, halting the drift. This might be stable, except that:

7) In the Indian Ocean, the seasonal (monsoonal) Somali Current (±20 Sv, Lee and Marotzke 1997) and the southward-flowing Agulhas current (a 65-Sv western boundary current, analogous to the Gulf Stream, driven by the ocean-wide southern-hemisphere wind curl) prevent the formation of a western warm pool. The monsoon cycle permitting, a convection center forms more-or-less centrally.

8) The Indian convection center drifts eastward at 3 cm/second (250 km/day);

9) When it reaches Indonesia, the Indian Ocean organizes another central convection center, repeating this process to form the MJO with its 30-90–day cycle.

10) Conditions in Indonesia permitting, the convection center, and some fraction of its accompanying warm water, make it through Indonesia to add its water to the Pacific Warm Pool.

11) This 'Indonesian Throughput' may become a Kelvin wave that expands the Pacific Warm Pool.

12) When the Warm Pool is fully developed, the next Kelvin wave to be triggered (usually by something with a strong seasonal component) will bring the warm water of an El Niño to the eastern Pacific.

Draining the Warm Pool

There are 2 distinct appearances to an El Niño. These are:

1) Westward motion of warm surface water (See Figure 9). Warm water appears first in the east and is progressively uncovered by upwelling (Rasmussen and Carpenter 1982). This is the classical 'fisherman's' view of events.
2) Eastward motion of warm surface (See Figure 4). Warm water spreads eastward from the Warm Pool toward the coast. This appears to be the customary satellite view of events. Figure 7 shows something similar happening at the depth of the EUC.

Is this what Delecluse et al. (1998) mean when they say "more than one mechanism is active in the generation and evolution of ENSO events"? Probably not: Billy Kessler of PMEL/Seattle provided the currently accepted understanding of Warm Pool drainage in an e-mail tutorial. I paraphrase:

Both eastward and westward-developing El Niños can be explained by equatorial wave dynamics, when the preceding situation is taken into account. Although wave advection contributes to SST, the primary mechanism of warming in the east is that Kelvin waves deepen the thermocline, making upwelling less efficient at cooling the surface. Surface cooling requires that upwelling reach cooler water below the thermocline: even strong upwelling will not cool the SST if it brings up only warm water.

An example: In late 1997, winds east of 120°W – and the upwelling they induced – remained normal, Kelvin waves (measured at 110°W) were eastward at times, but insufficient to account for the 4° warming in mid-1997 (Kessler, Deep-Sea Res. in review). Yet the SST warmed dramatically as the thermocline deepened, and there seems no doubt that the wave-deepened thermocline removing the source of cool water was the cause. Otherwise it is hard to explain eastern warming while local winds and clouds remained normal.

"The result is that the effect of upwelling on SST is a mix of local and remote effects, and where the initial warming appears and the direction of its spread will depend strongly on the initial shape of the thermocline."

Modelling ENSO

The starting points of any attempt to model ENSO are Cane and Sarachik (1983) on equatorial oceanography and McCreary (1985) on equatorial dynamics.

ENSO has all of the attributes which attract modellers: it is economically important, quasi periodic, of a size within reach of work stations rather than supercomputers, and there is some data. Thus it is the single most extensively modelled climatic feature. I once thought to include a directory, with models classified by type, but there are too many, and the number grows so rapidly, that it seems pointless. Many can be found with simple searches on the Internet. It is, however, still useful to distinguish between the various types of models.

Model Types

Linear shallow-water equatorial-ocean models, despite their simplicity, are understandable and so have contributed greatly to ENSO theory.

The next level of complexity, intermediate-coupled models (ICMs) with a non-linear atmosphere coupled to the shallow-water ocean, must parametrize many features. The earliest ICM by Cane and Zebiak (1985) (CZ) was limited to the tropical Pacific. Hampered by inadequate data, it nevertheless captured many important features of ENSO, and provided the first successful forecasts from a physical (rather than a historical-statistics) model. Initialized with a 4-month-long, 2-m/s westerly wind anomaly in the western Pacific, it thereafter oscillated slightly more regularly than ENSO itself during a 90-model-year run, indicating the existence of a natural mode to the system.

Other ICMs differ largely in details of interest only to modellers. Careful parameterization of all processes – that is, reducing them to single numbers – which affect SST is critical, but the important atmospheric convection is notoriously difficult to parametrize.

The equations of an ICM are simple. Such models often try to reduce the world to 3 numbers:

Scaled wind stress per unit SST anomaly, which determines atmospheric feedback;

Adjustment-time constant, which is the ratio of ocean to atmospheric relaxation;

Surface-layer coefficient, which controls feedback from the thermocline.

Other effects which must still be parametrized are clouds, which intercept incoming heat. The timing, location, height, and type of clouds, are all important. Even the cloud-drop-size distribution matters, because of the strong dependence of optical scattering on drop diameter. All effects of cloudiness are frequently reduced to a single number, the albedo. Perhaps the most useful purpose served by ICMs is to show the true complexity of the real world.

The most complex models are large Coupled ocean-atmosphere General-Circulation Models (CGCMs), which attempt to model the atmosphere and an entire ocean. These are expensive to run, yet still require parametrization to include effects not modelled directly. Cane et al. (1997) found that air-sea coupling in GCMs was less than in nature, because GCMs are run at too coarse a resolution to resolve equatorial dynamics.

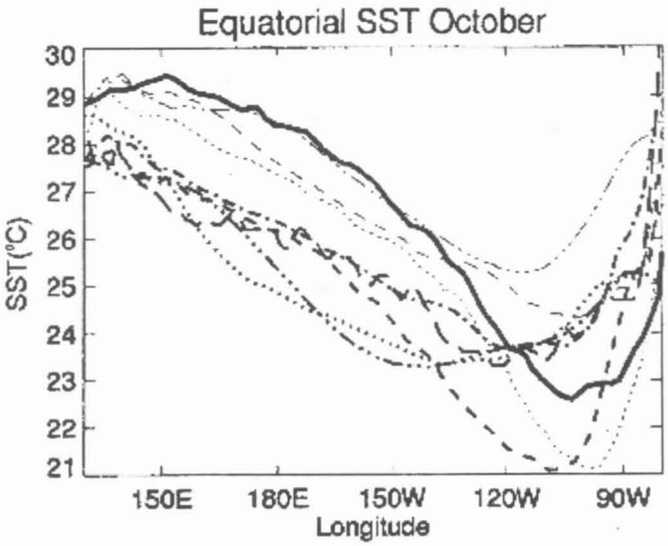

Figure 13. Comparison of equatorial SST by 8 CGMs. The heavy line is observed temperature. Despite general agreement, 1°C is a large error and indicates that the model is still unrealistic. (from Delecluse et al. 1998.)

Vertical velocities were too small and the thermocline too diffuse, reducing the effect of wind change on heat flux just where the Earth absorbs most of its heat. The net result was to overlook a considerable equatorial contribution to delaying (and regulating) global warming. This in turn underestimated the longer term probability of strengthening ENSO teleconnections, with substantial economic and social consequences. (The initial highly publicized overestimates of global warming, and their later reduction by better models, has been seized upon by oil companies and politicians as an excuse to refuse limitations on greenhouse-gas production.)

The end result is that as Figure 13 shows, even CGCMs cannot yet reproduce observed Pacific equatorial SSTs with the accuracy needed for reliable modelling.

Comparing the behavior of 3 CGCMs, Février et al. (2000) concluded that "some of the physics is not correctly represented in the oceanic models". This is no surprise to modellers, whose question is always how best to handle the complexities which must be simplified to obtain any solution at all.

Prediction of El Niños

The first attempts to model ENSO events, and thus predict them, projected historical time series into the future (Houghton et al. 1996). As with the stock market predictions (and for much the same reason), they were not overly successful and did not forecast the 1982 El Niño.

An upgrade of the CZ model (Cane et al. 1986) successfully predicted the 1986 El Niño. However, it failed to predict the 1997 event, which was forecast by more comprehensive models (Stockdale et al. 1998). Yet even this forecast 'challenge [d] existing theories' missed both the inception and termination of the 1997 event (McPhaden 1999).

Baker-Blocker and Bouwer (1984) inject caution. The large range of frequencies in an ENSO time series leads them to suggest that 'large random pulses may serve as triggers to change atmospheric quasistable states, and may be either volcanic or solar in origin' – features well outside the scope of models.

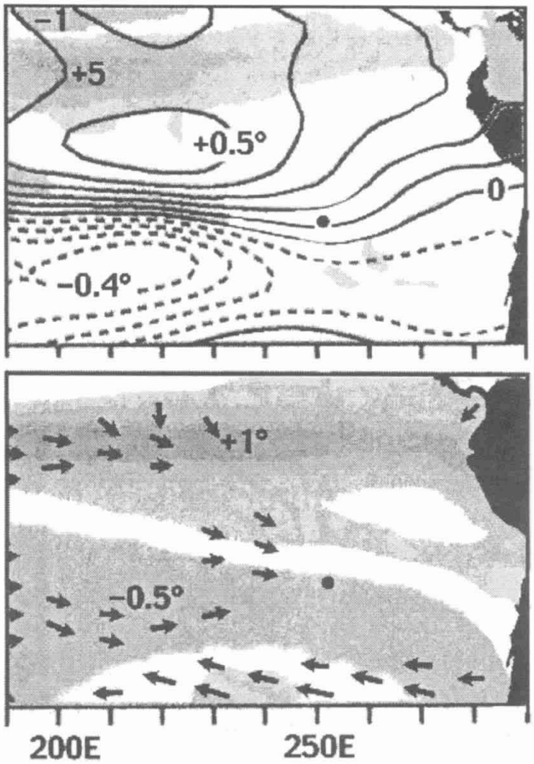

Figure 14. Climate variability derived from the TOGA array and NCEP/NCAR reanalysis, 1985–1993. All data are per standard deviation of the 'cold tongue index', yet another variant of the El Niño index. Top: Shading is atmospheric temperature/°C; contours are rainfall/cm. Bottom: Shading is SST/°C, vectors are surface wind. The vectors are, roughly, 2m/s in length. Rapa Nui (the black dot) lies at a relative minimum of all anomalies. (after Wallace et al. 1998.)

Looking Back, Looking Ahead

Interannual variability at Rapa Nui

The classic statement of knowledge about Rapa Nui and climate change is from Ropelewski and Halpert (1987), who succinctly say, "Insufficient station data for analysis" (see also Philander 1990). However, this situation is changing. Wallace et al. (1998) show anomaly maps of the major climatic variables – rainfall, tropospheric and sea-surface temperature, sea-level pressure, and surface wind – over the period 1985 through 1993. While this period lay between the major ENSO events of 1982 and 1997, the Central Pacific was still noticeably affected.

Figure 14 summarizes the maps of Wallace et al., showing climate variability in the south eastern Pacific derived from 8 years of TOGA data and a reanalysis including satellite data by the National Center for Atmospheric Research (NCAR). The numbers are scaled by the standard deviation of the 'cold tongue index' (deviation from the mean temperature over the area 6°N–6°S, 180°E–270°E, a modified El Niño Index). The 140-year range of this index is, roughly, –1° to +2°. The authors do not give a number for the standard deviation, but it appears to be about 0.5°C, meaning that values in Figure 14 should be multiplied by 2. Once again, we find Rapa Nui, marked by the dot, lying very near regions of zero change. It appears that Rapa Nui has one of the most equable climates on Earth.

It is significant that none of the anecdotes relating bad consequences from the 1997 El Niño (MacIntyre 1999) came from Rapa Nui. Can any reader recall something that should be brought to the attention of climatologists? This was the largest El Niño of the century (and presumably of the millennium). If no one on Rapa Nui noticed it, perhaps no one noticed earlier events either.

So far, the most important consequence of ENSO on Polynesian settlement might be the reversal of trade winds in western Polynesia and their weakening in the east, an effect which extends to the Date Line more or less regularly. This make eastward canoe voyaging periodically easier near the equator – a pattern surely known and used by the Polynesians.

ENSO and the Greenhouse

A preview of future Rapa Nui climate might be gleaned from a model which shows an 'El Niño-like response' of the Pacific to a doubling of greenhouse CO^2. Under such conditions, the NCAR CGCM shows a 3°C temperature rise for Rapa Nui, with no change in precipitation (Meehl and Washington 1996). Can this result be turned around and interpreted as similar to past El Niños?

With no change in rainfall, would a 3-year, 3°C temperature rise have disrupted the 16th-century society of the Rapanui? It would scarcely affect people directly. The effect on plants is more problematical and deserves the attention of specialists.

Yet a 3°C rise from an El Niño would be unlikely. The GCGM runs the model to equilibrium with doubled CO^2, requiring many decades of model time, during which the entire surface ocean also comes to a new equilibrium. This is not what happens during an El Niño, which is only a transient displace-

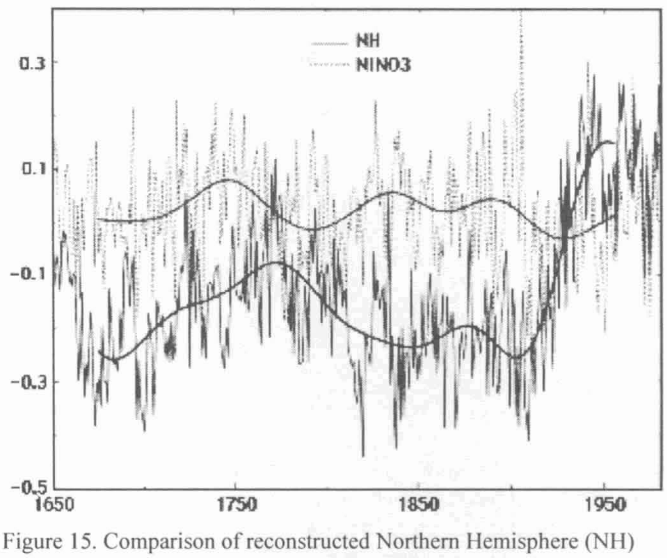

Figure 15. Comparison of reconstructed Northern Hemisphere (NH) mean annual temperature and the (scaled) NINO3 index. The smooth lines are 50-year running means; the apparent downturn in NH in 1950 is a sinusoidal oscillation on a continuing rise (from Mann et al. 2000).

ment of equatorial water. The Central South Pacific Ocean is one of the world's largest temperature buffers, and will not be greatly affected by 3-year transients. It would surprise me if a 3-year El Niño caused an 0.5° mean-temperature change at Rapa Nui.

Our real interest in the effects of ENSO on Rapa Nui was the hope that they might provide a clue about the effects of a more general climate change. Perhaps the lack of ENSO-related effects is itself such a clue.

The best answer we have to this question is still indirect. We have found little climatic connection between ENSO and Rapa Nui, and in Figure 15, we see a convincing lack of coupling between ENSO and the global mean temperature. Actually, NH in Figure 15 is the northern hemisphere mean, because that's where we have the best historical reconstructions. The 0.6°C increase in NH since 1900 is the long anticipated response to anthropogenic CO^2, and it seems to have had no effect whatsoever on ENSO.

Figure 15 does not speak directly to the '13th-century event' of Nunn (1999), which he sees as disrupting societies across tropical Polynesia (although one must note that he uses '13th century' very broadly). But it does suggest that one must examine Rapa Nui itself for any climatic consequences. The most likely influence of mean temperature on ENSO is to change the frequency and perhaps duration of El Niños, rather than the area affected. Since El Niños themselves seem to have little effect on Rapa Nui, climate changes like the Little Ice Age – so noticeable in Northern Europe – might not be noticed even by a climatologist on Rapa Nui.

Conclusions

This review does not support the hypothesis of significant ENSO-related interannual climate variability at Rapa Nui. Once again in Figures 9 and 14, Rapa Nui lies almost exactly on the line of zero effect.

The position of Rapa Nui at the center of the SE Pacific High appears to isolate it from the major sources of interannual climate variability. The idea of an ENSO-related climatic trigger which toppled a society on the verge of trouble is less tenable than it once was.

Climatic equability does not prevent exceptional events which might afflict a society, some of which (severe storms?) could be weather related. Such disasters may be less serious to a culture with minimal infrastructure than they seem to us, where they can destroy a whole range of essential technological supports that the Rapanui never had. In any case, the archaeological evidence suggests chronic stress rather than trauma.

It seem increasingly likely that Rapa Nui provides a positive answer to E. O. Wilson's (1993) question, 'Is humanity suicidal?', by supplying a recent example of anthropogenic ecodestruction followed by civil strife, cannibalism, and the loss of 2/3 of the population (Bahn and Flenley 1992, MacIntyre 1999).

Acknowledgements

I gratefully acknowledge discussions with both of Ireland's physical oceanographers, Peter Bowyer and Martin White, e-mail discussions with David Pierce at SIO, Roman Glazman at JPL, Meghan Cronin and Michael McPhaden at PMEL, and tutorials from William Kessler at PMEL. Georgia Lee, as always, provided insights into things Rapa Nui.

References

Allan, R. J. 2000. ENSO and climatic variability in the past 150 years. *El Niño and the Southern Oscillation: Multiscale Variability and its Impacts on Natural Ecosystems and Society.* H. E. Diaz and V. Markgraf, eds.: 3–55. Cambridge University Press.

Allan R., J. Lindesay and D. Parker. 1996. *El Niño - Southern Oscillation and Climatic Variability.* CSIRO Publishing.

Bahn, P. G. and J. Flenley. 1992. *Easter Island, Earth Island.* Thames and Hudson, London.

Baker-Blocker, A. and S. D. Bouwer. 1984. El Niño: Evidence for climatic nondeterminism? *Archives for Meteorology, Geophysics, and Bioclimatology* B34:65-73.

Barnett T. P. 1983. Interaction of the Monsoon and Pacific Trade-wind System at Interannual Time Scales. I. The equatorial zone. *Mon. Weather Review* 111:756-773.

Battisti, D. S. and A. C. Hurst. 1989. *J. Atmos. Sci.* 46:1687-1712.

Bjerknes, J. 1966. A possible response of the atmospheric Hadley circulation to equatorial anomalies of mean temperature, *Tellus* 18: 820-829.

Bjerknes, J. 1969. Atmospheric Teleconnections from the Equatorial Pacific. *Monthly Weather Rev.* 97:163-172.

Cane, M. A.and E. S. Sarachik. 1983. Equatorial Oceanography. *Rev. Geophys.* 21:1137-1148.

Cane, M. A. and E. Zebiak. 1985. A theory for El Niño and the Southern Oscillation. *Science* 228:1085-1087.

Cane, M. A., E. Zebiak and S. C. Dolan. 1986. Experimental forecasts of El Niño. *Science* 231:827-832.

Cane, M. A., A. C. Clement, A. Kaplan, Y. Kushnir, D. Pozdnyakov, R. Seager, S. E. Zebiak and R. Murtugudde. 1997. Twentieth-century sea-surface-temperature trends. *Science* 275:957-960.

Cronin, M. F. and M. J. McPhaden. 1998. Upper ocean salinity balance in the western equatorial Pacific. *J. Geophys. Res.* C103:27567-27587.

Davis, M. 2000. *Late Victorian Holocausts: El Niño, Famines, and the Making of the Third World.* Verso, London.

Delcroix, T., B. Dewitte, Y. duPenhoat, F. Masia and J. Picaut. 2000. Equatorial waves and warm pool displacements during the 1992-1998 El Niño Southern Oscillation events: Observations and modelling. *J. Geophys. Res.* C105:26045-26062.

Delecluse, P., M. K. Davey, Y. Kitamura, S. G. H. Philander, M. Suarez and L. Bengtsson. 1998. Coupled general-circulation modelling of the tropical Pacific. *J. Geophys. Res.* C103:14,357–14,373.

Fagan, B. 1999. *Floods, Famines and Emperors: El Niño and the Fate of Civilizations.* Basic Book, New York.

Février, S., C. Frankignoul, J. Sirven, M. K. Davey, P. Delecluse, S. Ineson, J. Macias, N. Sennéchael and D. B. Stephenson. 2000. A multivariate intercomparison between three oceanic GCMs using observed current and thermocline depth anomalies in the tropical Pacific during 1985-1992. *J. Mar. Sys.* 24:249-275.

Harrison, D. E. and N. K. Larkin. 1998. El Niño-Southern Oscillation sea-surface temperature and wind anomalies, 1946-1993. *Rev. Geophys.* 36:353–399.

Hayes, S. P., J. M. Toole and L. J. Mangum. 1983. Water-mass and transport variability at 110°W in the Equatorial Pacific. *J.Phys. Oceanogr.* 13:153–168.

Hénin, C., Y. duPenhoat, and M. Ioualalen. 1998. Observations of sea surface salinity in the western Pacific fresh pool: Large-scale changes in 1992-1995. *J. Geophys. Res.* C103:7523–7536.

Houghton, J.T., L.G. Meira Filho, B.A. Callander, N. Harris, A. Kattenberg, K. Maskell eds. 1996. *Climate Change 1995, The Science of Climate Change, Summary for Policy Makers, Intergovernmental Panel on Climate Change.* Cambridge University Press, Cambridge.

Jin, F.-F., J. D. Neelin and M. Ghil. 1996. El Niño/Southern Oscillation and the annual cycle. Subharmonic frequency locking and aperiodicity. *Physics* D98:442-4521.

Johnson, G. C., M. J. McPhaden, G. D. Rowe and K. E. McTaggart. 2000. Upper equatorial Pacific Ocean current and salinity variability during the 1996-1998 El Niño - La Niña cycle. *J. Geophys. Res.* C105:1037-1053.

Kerr, R. A. 1999. Big El Niños ride the back of slower climate change. *Science* 283:1108–1109.

Kessler, W. S. 1991. Can reflected extra-equatorial Rossby waves drive ENSO? *J. Phys. Oceanography* 21:444-452.

Lee, T., and J. Marotzke. 1997. Inferring meridional mass and heat transorts of the Indian Ocean by fitting a general-circulation model to climatological data. *J. Geophys. Res.* C102:28,932–28,943.

Lorenz, E. N. 1963. Deterministic Non-periodic Flow. *J. Atmos. Sci.* 20:130-141.

Luther, D. S., D. E. Harrison, and R. A. Knox. 1983. Zonal winds in the central equatorial Pacific and El Niño. *Science* 222:327-330.

McCreary, J. P. 1985. Modelling equatorial ocean circulation. *Rev. Fluid Mech.* 17:359-409. [Dated, but the place to begin].

MacIntyre, F. 1999. 'Is Humanity Suicidal?': Are there clues from Rapa Nui? *Rapa Nui Journal* 13: 35-41.

MacIntyre, F. 2001. ENSO, climate variability, and the Rapanui: 1. The basics. *Rapa Nui Journal* 15:17–26.

McPhaden M. J. 2000. El Niño and La Niña: Causes and Consequences. *Wiley Encyclopedia of Global Environmental Change.*

McPhaden, M. J., A. J. Busalacchi, R. Cheney, J.-R. Donguy, K. S. Gage, D. Halpern, M. Ji. P. Julian, G. Meyers, G. T. Mitchum, P. P. Niiler, J.Picaut, R. W. Reyolds, N. Smith, K. Takeuchi and U. T. Cobleigh. 1998. The Tropical Ocean-Global Atmosphere observing system: A decade of Progress. *J. Geophys. Res.* C103: 14,169–14,240.

McPhaden, M. 1999. Genesis and evolution of the 1997-98 El Niño. *Science* 283:950–954.

McPhaden, M. J. and J. Picaut. 1990. *Science* 250:1385–1388.

Madden, R. A. and P. R. Julian. 1971. Detection of a 40-50 day oscillation in the zonal wind in the tropical Pacific. *J. Atmos. Sci.* 28:702–708.

Madden, R. A. and P. R. Julian. 1972. Description of global-scale circulation cells in the tropics with a 40-50–day period. *J. Atmos. Sci.* 29:1109–1123.

Maes C. 2000. Salinity variability in the equatorial Pacific Ocean during the 1993–98 period. *Geophys. Res. Lett.* 27:16591–662.

Mann, M. E., R. E. Bradley, and M. K. Hughes. 2000. Long-term variability in the El Niño/Southern Oscillation and associated teleconnections. *El Niño and the Southern Oscillation: Multiscale Variability and its Impacts on Natural Ecosystems and Society.* H.Diaz and V. Markgraf, eds.,:357-412. Cambridge University Press.

Mantua, N. J. and D. S. Battisti. 1995. *J. Climate* 8:2897–2927.

Meehl, G. A. and W. M. Washington. 1996. El Niño-like climate change in a model with increased atmospheric CO2 concentrations. *Nature* 382:56-60.

Niiler, P. .P, A. Sybrandy, K. Bi, P. Poulain and D. Bitterman. 1995. Measurements of the water-following capability of Holey-sock and TRISTAR drifters. *Deep-Sea Res.* Part 1, 42:1951–1964.

Nunn, P.D., 1999. *Environmental Change in the Pacific Basin: Chronologies, Causes, Consequences.* Wiley, London.

Ortlieb, L. 2000. The documented historical record of El Niño events in Peru: An update of the Quinn Record (sixteenth through nineteenth centuries). *El Niño and the Southern Oscillation: Multiscale Variability and its Impacts on Natural Ecosystems and Society.* H. E. Diaz and V. Markgraf, eds.:207–295. Cambridge University Press.

Penland, C., and T. Magorian. 1993. Prediction of Niño 3. Sea-surface temperatures using linear inverse modeling. *J. Clim.* 6:1067–1076.

Philander, S. G. H. 1990. *El Niño, La Niña, and the Southern Oscillation.* Academic Press, New York,.

Picaut, L., M. Ioualalen, C. Menkes, T. Delcroix and M. J. McPhaden. 1996. Mechanism of the zonal displacements of the Pacific Warm Pool: Implications for ENSO. *Science* 274:1486-1489.

Picaut, J., F. Masia, and Y. du Penhoat. 1997. An advective-reflective conceptual model for the oscillatory nature of ENSO. *Science* 277:663–668.

Quinn, W. H., and V. T. Neal. 1983a. Long-term variation in the Southern Oscillation, El Niño, and Chilean subtropical rainfall. *Fishery Bull.* 81:363–374.

Quinn, W. H. and V. T. Neal. 1983b. Southern Oscillation-related climatic changes and the 1982-1983 El Niño. *Proc. Internat. Conf. on Marine Resources of the Pacific* (Santiago). P.M. Arana, ed. :71-82.

Rasmussen, E. M. and T. H. Carpenter. 1982. Variations in the tropical sea-surface temperature and surface wind fields associated with the Southern Oscillation/El Niño. *Mon. Weather Rev.* 110: 354–384. [or 517-528]

Ropelewski, C. F. and M. S. Halpert. 1987. Global and regional scale precipitation patterns associated with the El Niño/Southern Oscillation. *Mon. Weather Rev.* 115:1606–1626.

Schopf, P. S. and M. J. Suarez. 1988. A delayed action oscillator for ENSO. *J. Atmos. Sci.* 45:3283-3287.

Shaw, R. 1984. *The Dripping Faucet as a Model Chaotic System.* Aerial Press, Santa Cruz.

Stockdale, T., A. J. Busalacchi, D. E. Harrison, and R. Seager. 1998. Ocean modeling for ENSO. *J. Geophys. Res.* C103:14,325–14,355

Tziperman, E., M. A. Cane, S. E. Zebiak, Y. Xue and B. Blumenthal. 1996. Locking of El Nino's peak time to the end of the calendar year in the delayed oscillator picture of ENSO. *J. Climate* 11:2191–2199.

Tziperman, E., S. E. Zebiak and M. A. Cane. 1997. Mechanism of seasonal-ENSO interaction. *J. Atmos. Sci.* 54:61-71.

Verschell, M. A., J. C. Kindle, and J. J. O'Brien. 1995. Effects of Indo-Pacific throughflow on the upper tropical Pacific and Indian Oceans. *J. Geophys. Res.* C100:18,409–18,420.

Wallace, J. M., E. M. Rasmusson, T. P. Mitchell, V. E. Kousky, E. .S. Sarachik, and H. von Storch. 1998. On the structure and evolution of ENSO-related climate variability in the tropical Pacific: Lessons from TOGA. *J. Geophys. Res.* C103:14,241–14,259.

Webster, P. J. and T. N. Palmer. 1997. The past and future of El Niño. *Nature* 390:562-564.

Wilson, E. O. 1993. Is humanity suicidal? *BioSystems* 31:235-242.

Wyrtki, K. 1975. El Niño – the dynamic response of the equatorial Pacific Ocean to atmospheric forcing. *J. Phys. Oceanog.* 5:572–584.